

LISBET: a self-supervised Transformer model for the automatic segmentation of social behavior motifs

Giuseppe Chindemi*, Benoit Girard* and Camilla Bellone
Department of Basic Neurosciences, University of Geneva, Switzerland

Corresponding authors: camilla.bellone@unige.ch; giuseppe.chindemi@unige.ch

Abstract

Social behavior, defined as the process by which individuals act and react in response to others, is crucial for the function of societies and holds profound implications for mental health. To fully grasp the intricacies of social behavior and identify potential therapeutic targets for addressing social deficits, it is essential to understand its core principles. Although machine learning algorithms have made it easier to study specific aspects of complex behavior, current methodologies tend to focus primarily on single-animal behavior. In this study, we introduce LISBET (seLf-supervised Social BEhavioral Transformer), a model designed to detect and segment social interactions. Our model eliminates the need for feature selection and extensive human annotation by using self-supervised learning to detect and quantify social behaviors from dynamic body parts tracking data. LISBET can be used in hypothesis-driven mode to automate behavior classification using supervised finetuning, and in discovery-driven mode to segment social behavior motifs using unsupervised learning. We found that motifs recognized using the discovery-driven approach not only closely match the human annotations but also correlate with the electrophysiological activity of dopaminergic neurons in the Ventral Tegmental Area (VTA). We hope LISBET will help the community improve our understanding of social behaviors and their neural underpinnings.

Introduction

Animal behavior has been traditionally categorized and labeled based on human identification of stereotypical movements or actions. Recently, the rise in popularity of machine learning methods in biological disciplines has provided behavioral researchers with novel tools that are revolutionizing the whole field. These algorithms serve a dual purpose: firstly, they replicate human annotations through a hypothesis-driven approach (Bohnslav *et al.*, 2021; Marks *et al.*, 2022); secondly, they find new motifs through a discovery-driven approach (Wiltschko *et al.*, 2020; Dunn *et al.*, 2021; Hsu and Yttri, 2021; Luxem *et al.*, 2022).

However, most progress in the field has been made in single-animal settings. Social interactions are characterized by the interplay of multiple individuals and introduce greater challenges. While single-animal actions can be deconstructed into simple features like velocity (i.e., locomotion) or body part's positions (i.e., rearing), social interactions span multiple timescales and can be of extreme complexity (i.e., group dynamics during hunting). Classification approaches based on hand-made rules or supervised learning methods have shown promising results in specific social scenarios, such as physical contact or chasing (de Chaumont *et al.*, 2019; Nilsson *et al.*, 2020; Segalin *et al.*, 2021; Marks *et al.*, 2022; Ye *et al.*, 2023), but they still offer limited generalization to novel conditions.

Furthermore, these approaches introduce anthropomorphic bias and can hardly capture the extensive spectrum of social behaviors exhibited by animals.

To address these challenges, we developed a self-supervised Social Behavioral Transformer (LISBET) model for the automated discovery and classification of social behavior motifs from body points coordinates obtained by tracking video recordings of mice pairs. LISBET is based on the ViT/ViViT architectures (Dosovitskiy *et al.*, 2020; Arnab *et al.*, 2021) and trained to produce an embedding of the scene by solving four self-supervised learning tasks. LISBET uses the body point coordinates of the mice as input, obtained using any pose estimation tracking software such as DeepLabCut (Mathis *et al.*, 2018) or MARS (Segalin *et al.*, 2021). Our findings demonstrate that, post-training, LISBET can: (1) extract key features of social behaviors and classify them to mirror human annotations using a hypothesis-driven approach; (2) use a discovery-driven approach to detect and segment social behavior motifs without prior examples. Finally, motifs from the discovery-driven approach not only align closely with human annotations but also correlate with the electrophysiological activity of VTA dopaminergic neurons recorded in vivo in freely moving animals.

Code and weights of the best-performing LISBET models will be made publicly available and could be used by the community to automate social behavior annotation, individual stratification, or to study novel experimental conditions hypothesis-free.

Results

Human annotations align LISBET embeddings.

LISBET is a model based on ViT/ViViT transformer architectures (Dosovitskiy *et al.*, 2020; Arnab *et al.*, 2021), designed to analyze video recordings of social behavior in animal experiments. The model operates on coordinates of animal body parts (i.e., key points) using a sliding window over a video. This format has increasingly been adopted in behavioral neuroscience due to its computational efficiency and potential for standardization (Mathis *et al.*, 2018; Pereira *et al.*, 2020; Pereira, Shaevitz and Murthy, 2020; Dunn *et al.*, 2021; Segalin *et al.*, 2021). Each window is processed by a frame encoder, transforming it into an intermediate representation. Then, a position encoding is added to the frame representation, and the resulting tokens are introduced to a transformer encoder to generate the final “LISBET embedding”. This embedding is a feature vector that encodes a compressed representation of the ongoing scene and can be used to solve user-specified tasks, including behavior classification or segmentation (Fig. 1a).

To train LISBET without relying on human-annotated examples, we designed four self-supervised tasks using videos from the unlabeled tracking dataset provided in CalMS21 (Sun *et al.*, 2021) (Fig. 1b). In brief, this dataset contains the coordinates corresponding to seven body parts of two mice, during a resident-intruder paradigm. We analyzed a window of 200 frames prior to each given frame. The coordinates were recorded at a rate of 30 frames per second. To identify the optimal model hyperparameters, we used grid search and a 4-fold cross-validation (Supplementary Fig. S1 and Supplementary Table S1).

The training tasks were conceived to highlight the most salient aspects of social interactions. The first task, “Swap Mouse Prediction (SMP)”, requires the model to predict whether the given input window is an authentic video segment or an artifact generated by selecting the body part coordinates of two mice from different videos. The second task, “Next Window Prediction (NWP)”, requires the model to distinguish whether two successive input windows are extracted from the same video or whether the second one is randomly sampled. The third task, “Video Speed Prediction (VSP)”, requires the model to predict whether the sampling rate of an input window corresponds to the original one. Finally, the

fourth task, “Delay Mouse Prediction (DMP)”, requires the model to determine whether the mice presented in an input window are aligned in time or artificially delayed one another.

To test the performance of the model to capture social interactions, we trained a linear classifier to predict the human-annotated behaviors (attack, mount, investigate) in the CalMS21 - Task 1 dataset (Sun *et al.*, 2021). While the weights of the LISBET backbone were frozen, we found that the model obtained an F1-score = 0.71. Subsequent fine-tuning of the entire model improved the classifier, getting an F1-score = 0.78. Notably, fitting the model without pre-training the backbone achieves an F1-score = 0.74, highlighting the importance of the self-supervised pre-training. Using UMAP-reduced dimensions, we visualized clusters of LISBET embedding overlapping with human annotations (Fig. 1c).

To further investigate the generalization power of LISBET embeddings, we performed a similar analysis using the CalMS21 - Task 3 dataset (Sun *et al.*, 2021). This dataset is characterized by a smaller training set of seven rare behaviors. The model obtained an average F1-score = 0.25 despite only the linear classifier weights being available for training. Fine-tuning the model improved the classifier performance to F1-score = 0.29. We found that the clusters mirrored human-annotated behaviors, further demonstrating LISBET applicability in capturing social behavior (Fig. 1d).

In conclusion, LISBET successfully extracts features of social interaction without the need for human annotations. Furthermore, after fine-tuning, the model can automate human annotation.

Social behavior motifs discovery using LISBET embedding.

Traditional methods for the analysis of social interactions are inherently hypothesis-driven. While LISBET can automate human annotation, it also provides a novel approach for discovery-driven behavior analysis. We used a Hidden Markov Model (HMM) to segment the LISBET embedding of the CalMS21 Task 1 dataset (Fig. 2a) without relying on human annotations. The LISBET embeddings served as observations for the HMM. Each hidden state corresponds to a specific behavior inferred from the observations. Through this method, the HMM unravels the sequential organization of behavior, pinpointing the transition and duration of each identified state. We tested three different HMM models and decided to use an eight states model (HMM8), which successfully recovered the human labels (NMI = 0.33) and identified five new behavioral motifs (Fig. 2b). Interestingly, juxtaposing the LISBET embedding, human annotations, and HMM segmented motifs revealed a precise alignment (Fig 2c).

By analyzing the rate and the duration of the HMM-identified motifs, we found higher frequency for motif 1 (predominantly covering the “investigation” behavior) and longer bout-duration for motif 2 (aligning with mounting) as expected from the human annotation (Fig. 2e-f). Moreover, the analysis of transitions between motifs revealed number 4 as a central hub from which other motifs diverged (Fig. 2d).

These findings demonstrate LISBET's suitability for behavioral segmentation across varying levels of granularity. Moreover, these segmented motifs not only align closely with human annotations but also highlight recurrent sequential patterns of behaviors.

Automated social phenotype characterization

We have shown so far how LISBET can be used to quantify social interaction within an experimental group. Another interesting application of our model is group phenotyping (i.e., comparing different mouse lines or experimental conditions). To showcase this approach in the discovery-driven mode,

we compared the behavior of male mice when exposed to a mouse of the same versus opposite sex (Fig. 3a). We processed video recordings sourced from CRIM13 dataset (Burgos-Artizzu *et al.*, 2012), extracted body point coordinates via DeepLabCut (Mathis *et al.*, 2018) and generated social behavior features using LISBET. Subsequently, we segmented these features into eight distinct behavioral motifs using HMM (Fig. 3a). Analyzing LISBET embedding using UMAP, revealed the emergence of distinct motif clusters (Fig. 3a, left panel) and group clusters (Fig. 3a, right panel). Further analysis of the duration and rate of motif bouts exhibited significant differences between the groups (Fig. 3b-c). Transition analyses revealed distinct motif sequences, hinting at diverse behavioral strategies across sex interactions (Fig. 3d).

These findings demonstrate how LISBET can be used in a discovery-driven mode to characterize social phenotypes without relying on prior assumptions about the nature of the group-specific behaviors.

Neuronal correlates of social behavior

As LISBET motifs do not depend on human interpretation, we hypothesized that they could reveal the neural correlates of social interactions beyond the limited set of stereotypical behaviors commonly used in literature.

To test this hypothesis, we combined social interaction and electrophysiological recordings. Video acquisition of freely moving animals in dyadic interaction was obtained while concurrently recording spike unit activities of putative dopaminergic neurons in the Ventral Tegmental Area (VTA-pDA neurons) (Fig. 4a, top). Then, using DeepLabCut (Mathis *et al.*, 2018) and LISBET, we computed and segmented embeddings into sixteen motifs (Fig. 4a, bottom). While most motifs were not correlated with changes in neuronal activity (Fig. 4b, red for an exemplar motif) a few were correlated with diverging patterns of the VTA-pDA neuron activity (Fig. 4b, light and dark green for two exemplar motifs). In particular, motif three corresponded to an increase in activity, while motif eight corresponded to a decrease (Fig. 4b). Interestingly, the correlated motifs were part of longer action sequences, as shown by the transition matrix (Fig. 4c), and relatively frequent compared to the others (Fig. 4d-e), potentially indicating an ethologically relevant role of the observed neuronal activity.

Taken together, our results show that LISBET-derived motifs not only match human annotations but also align with specific neuronal activities.

Discussion

In this work we introduced LISBET, a transformer model for social behavior segmentation and classification. We have shown that training the model using four self-supervised tasks produces generalizable video embeddings suitable for behavior classification and phenotyping with no fine-tuning required. Finally, we used LISBET to segment the neural activity of VTA-pDA neurons based on the predicted behavioral motifs. Interestingly, we found that a few distinct motifs presented unique neuronal signatures despite being virtually indistinguishable using traditional analysis methods. Taken together, these findings suggest that LISBET can be used to expand the analysis toolkit of behavioral neuroscientists, minimizing the need for human-labeled data and drastically reducing the impact of the corresponding biases on the results.

Due to the use of body parts coordinates rather than direct video analysis, LISBET is a relatively small transformer model (less than 1.2 million free parameters for the backbone) with several important advantages. First, our model is suitable for deployment on home cage monitors and closed-loop systems. Second, it drastically simplifies the problem of merging data from different sources, as there is no need to account for recording parameters such as video luminance or

contrast. Last, it simplifies designing self-supervised learning approaches, as body part coordinates can be manipulated more easily than videos. However, directly using video recordings has its advantages and future studies could investigate that option.

The core strength of LISBET is its ability to capture key features of social behavior through its tailored self-supervised training tasks. We designed these tasks drawing inspiration from the literature on large language models (Devlin *et al.*, 2019) and on the key features of social behavior: the Swap Mouse Prediction task aimed at learning to pay attention to the spatial relationships between mice (i.e., trajectories crossings, mean distance and body parts orientation); the Next Window Prediction task was intended to learn to recognize repeated movement patterns over time (i.e., a series of attacks or mounting attempts); the Video Speed Prediction task was meant to aid the model learning the characteristic speed of each behavior in the videos (i.e., chasing is usually fast, investigation is usually slow); the Delayed Mouse Prediction sought to highlight the synchronicity of movements during social interactions (i.e., escaping because of a previous attack versus untriggered running).

The development of LISBET advocates for a paradigm shift in the analysis of social behavior. Traditionally tied to human interpretation, the domain has been held back by inherent biases, reproducibility challenges, the subjective nature and low temporal accuracy of annotations, and inconsistencies across annotators. These limitations hinder the characterization of neuronal correlates that underpin social behaviors. In contrast to traditional methods, LISBET ensures that behavioral data is extracted without these potential pitfalls. Additionally, our results elucidated LISBET's effectiveness in embedding social behaviors that are in close alignment with human annotations. The advantage of the self-supervised training becomes evident when contrasting the performance metrics (F1-scores) of the LISBET model before and after fine-tuning. In conclusion, LISBET eliminates the need for labor-intensive annotations, facilitates scalability, and reverses the conventional analysis process by shifting human interpretation to the last stages of the pipeline.

Using HMMs to segment LISBET embedding into distinct behavioral motifs complemented our unsupervised approach. First, it allows us to quantify the probability of observing a behavior based not only on the current observations but also on the previous states, potentially capturing a more complex sequence of social interactions. Second, it does not require human labels. Finally, fitting an HMM is a relatively inexpensive process. This approach allowed us to discover subtle behaviors overlooked by the annotators despite being at the same temporal resolution of human perception. Furthermore, using an automated scorer such as LISBET reduces the human annotation variability.

Comparing different groups based on the sole behaviors has been traditionally challenging. In addition to the pitfalls highlighted above, phenotyping required deeper stratification to capture the nuances of group-specific interactions. For example, disease models are often compared based on a few simple features, such as interaction time, which is rarely sufficient for meaningful stratification. In contrast, the analysis of LISBET motifs across granularity levels allowed us to easily distinguish between sex-specific interactions (male to female versus male to male).

However, while our findings are promising, this study has several limitations. First, in our study, we only considered pair interactions. Our model is not bound to a given number of animals, but extending it to include more than two animals is beyond the scope of this study. Furthermore, we chose the set of self-supervised training tasks based on intuition and successive iterations. While we were careful not to use the CalMS21 - Task 1 data for self-supervised training, the generalization power to this dataset was implicitly used as the success measure of the training procedure. For this reason, the self-supervised training tasks should not be considered as the absolute best choice for any possible mouse behavior but as an educated guess of what to look for in a video to recognize at least the most commonly investigated mouse behaviors. That is, other behaviors might have been better predicted using other self-supervised training tasks, emphasizing different aspects of mouse behavior.

However, our results show that the model can generalize to other datasets and behaviors (i.e. CalMS21 - Task 3, CRIM13, and our in-house dataset), supporting the choice of these tasks. Second, in this study, we did not consider complex social scenarios or species other than mice. We are currently investigating extensions of LISBET applied to human behavior, but research is still at an early stage. Third, our data pipeline is composed of three sequential steps, namely body-pose estimation, LISBET embedding, and HMM segmentation. Ideally, these steps could be concatenated to produce a true end-to-end solution, lowering the burden on the final user. This and other quality-of-life improvements are being developed over time, and we hope the open-source community will also be keen to be involved in the project. Fourth, while we found initial evidence of behavioral motifs correlation with neuronal activity, more research will be required to delve deeper into the precise neurological pathways and mechanisms that dictate these behaviors. Last, LISBET is a project under active development. To investigate and characterize the outcome of the model and its ethological relevance based on other behavioral features and human interpretation, we will need to convey to the final users the best practices for using the analysis pipeline.

In conclusion, LISBET paves the way for a more comprehensive, less biased, and discovery-driven approach to studying social behavior. By bridging the gap between human interpretations and behavioral intricacies and by highlighting potential neuronal correlates, it provides a valuable tool for both ethologists and neuroscientists. We believe that with the integration of tools like LISBET the future of social behavior analysis promises to be more nuanced and precise.

Methods

Software and Tools

LISBET was developed in Python (Van Rossum and Drake Jr, 1995), using TensorFlow (Martín Abadi *et al.*, 2015) and Keras (Chollet and others, 2015). The Hidden Markov Models (HMMs) were fitted using hmmlearn (hmmlearn, 2014). Dimensionality reduction for the visualization of the LISBET embeddings was performed using UMAP via umap-learn (McInnes, Healy and Melville, 2020). Standard scientific Python libraries were employed for data analysis, processing and visualization: numpy (Harris *et al.*, 2020), scipy (Virtanen *et al.*, 2020), pandas (McKinney, 2010), matplotlib (Hunter, 2007) and scikit-learn (Pedregosa *et al.*, 2011). Software development and data analysis were performed in the jupyterlab environment (Kluyver *et al.*, 2016).

Datasets

The CalMS21 dataset (Sun *et al.*, 2021) contains over one million frames from tracked videos, divided into three different annotation groups for the tasks of the MaBE 2021 competition: classic frame classification (Task 1), annotation style transfer (Task 2), and few-shot learning (Task 3). Furthermore, the dataset contains a set of 282 unlabeled videos (6 million frames). For more details, we refer the reader to the dataset reference (Sun *et al.*, 2021).

The CRIM13 dataset (Burgos-Artizzu *et al.*, 2012) consists of 88 hours of annotated videos. As the original dataset only provides tracking information for the body center of the animals, videos were re-tracked using DeepLabCut (Mathis *et al.*, 2018), following the same seven body parts configuration in the CalMS21 dataset (Sun *et al.*, 2021). Furthermore, videos were re-organized based on the metadata of the experiments (i.e. intruder sex and mouse line) to allow group comparisons in this study. Video segments containing only one animal or unsuccessfully tracked were excluded from the dataset. Where available, human annotations were verified and synchronized with the tracking data.

The VTA dataset was acquired in house using recorded videos of free social interactions. Body-pose estimation was extracted using DeepLabCut (Mathis *et al.*, 2018; Lauer *et al.*, 2022), following the same seven body parts configuration in the CalMS21 dataset (Sun *et al.*, 2021).

Transformer network architecture

The model backbone is adapted from the ViT architecture (Dosovitskiy *et al.*, 2020), akin to the factorized encoder proposed in ViViT (Arnab *et al.*, 2021). The frame encoder is a multi-layer perceptron (MLP) with GELU (Gaussian Error Linear Unit) activations. Positional encodings were learned during the training process and added to the frame embeddings.

Unlike ViT/ViViT, no special tokens were used to represent the class label or to separate different portions of the input in the transformer encoder. These tokens were not necessary as the number of body coordinates and window length are fixed. The function of the class token was implemented by adding a Max Pooling layer before the classification heads if required.

Classification heads were also implemented as MLPs, except for the linear decoders used to evaluate the generalization power of the LISBET embeddings compared to the human annotations from the CalMS21 datasets.

No dropout layers or other regularization techniques were used. All MLPs in the model have the same activation functions and hyperparameters.

Unless otherwise stated, the window size was 200 frames. We did not account for differences in the video frame rate, as all datasets used in this work were acquired at 25 or 30 frames per second.

Model fitting

The model was trained using four self-supervised learning tasks: Swap Mouse Prediction (SMP), Next-Window Prediction (NWP), Video Speed Prediction (VSP), and Delay Mouse Prediction (DMP). These tasks were defined as binary classification problems (i.e., original sequence vs altered sequence). At each training step, one example for each task was presented to the model backbone to compute the corresponding LISBET embedding and classified using a task-specific head. The backbone weights were shared across tasks. Model performance was calculated as binary accuracy. Label smoothing was used to improve generalization. The number of training epochs was determined during hyperparameter tuning.

Models for frame classification were either fine-tuned from a pre-trained LISBET embedding model (self-supervised) or trained from scratch as control cases. Frame classification was performed using a linear decoder and evaluated in terms of F1-score. For the CalMS21 dataset, the “other” class was excluded from the score calculations, as suggested by its authors (Sun *et al.*, 2021). Model evaluation was always performed on a held-out test set never used during training or hyperparameter tuning.

It should be noted that, at each epoch, the training and validation set are randomly generated from the source training and validation data. This implies that every epoch is unique compared to the actual input data, although the source sequences (i.e., body pose estimation data) used for each set are frozen and no data spillover is allowed.

Hyper parameters tuning

The main hyperparameters of the transformer model were chosen via a custom grid search:

- Embedding dimension in [16, 32, 64, 128],
- Number of layers and encoder heads in [2, 4, 8, 16],
- MLP hidden layer dimension in [512, 1024, 2048, 4096].

To reduce the computational cost of the search, 12 model configurations were chosen from the grid with a progressively increasing number of parameters. Each candidate was evaluated on 4 cross-validation splits of the training set (repeated random sub-sampling validation, 90/10 ratio of training over validation data). The model was trained for 100 epochs, as described in section “Model Fitting”, using the CalMS21 unlabeled dataset (Sun *et al.*, 2021). The performance of each configuration was assessed as the mean accuracy over the last 10 training epochs of the corresponding models across training tasks and cross-validation splits. The model with the highest score was chosen as the best candidate and re-trained on the whole training set.

Motifs segmentation

Motifs were segmented using a Gaussian Hidden Markov Model (Gaussian-HMM), fitted using the expectation-maximization (EM) algorithm. Model fitting was halted after convergence (delta log-likelihood < 0.01) or 500 EM steps. The number of hidden states was manually chosen for experiments focussing on data exploration and algorithmically estimated for fully automated experiments by iteratively increasing the model size until the gain in log-likelihood was negligible.

Data availability

The CalMS21 and CRIM13 datasets are available online on the website of their developers. The VTA dataset is available upon request to the authors. Analysis scripts and results will be publicly available soon.

Code availability

LISBET source code, documentation, and examples will be publicly available soon.

Figures

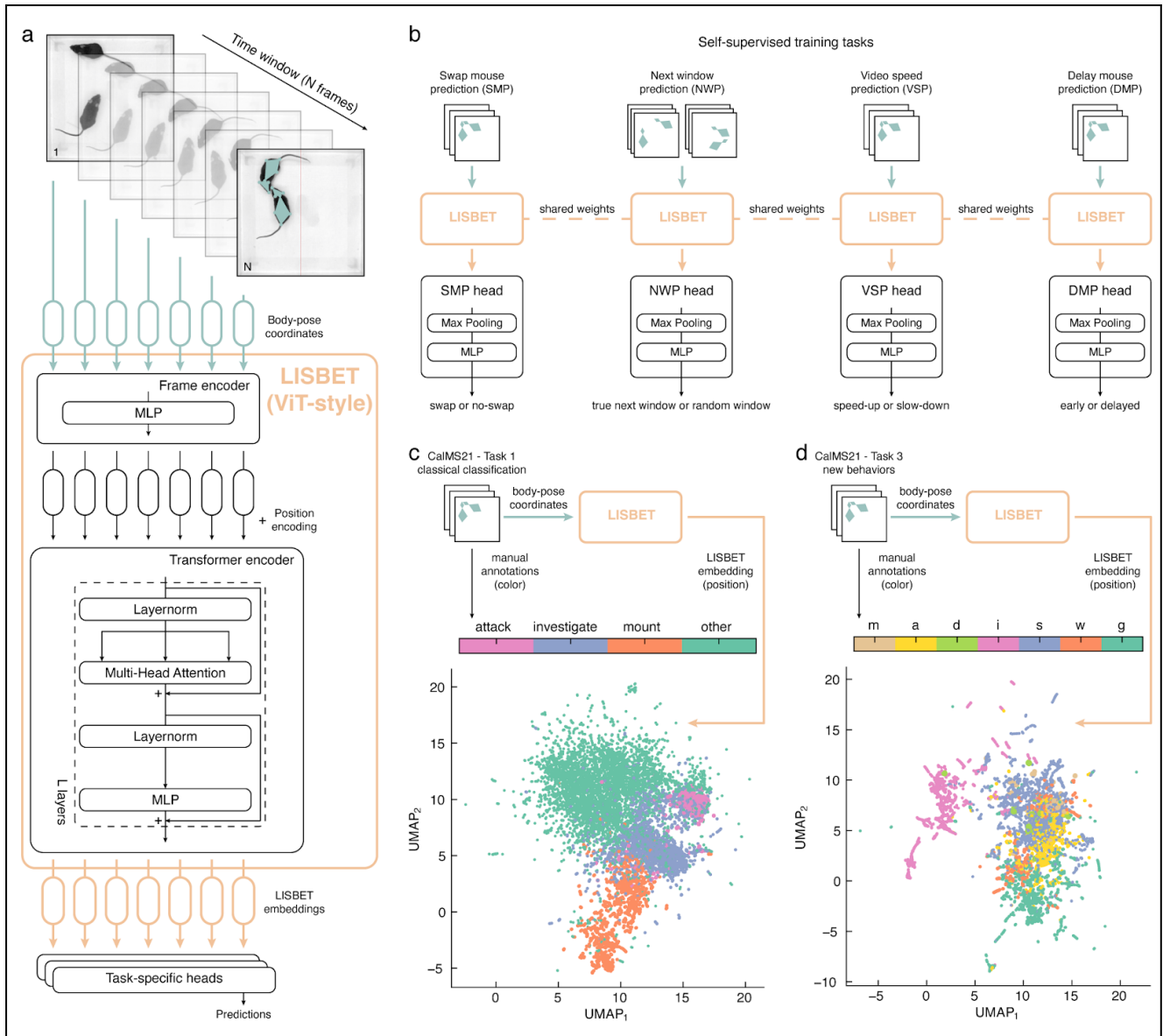


Fig. 1: LISBET architecture, self-supervised training, and comparison with human annotations. **a**, Schema of the LISBET backbone architecture. The input video is divided into sliding windows of N frames. Body-pose of mice in each window is encoded, frame by frame, using a Multi Layer Perceptron (MLP) layer. A learnable position encoding is added to the frame encoding before the transformer encoder (L sequential layers). **b**, Schema of the self-supervised training strategy. Four training tasks are sequentially solved using a shared LISBET backbone and four, task-specific, classification heads. Each head is composed of a Max Pooling Layer followed by a MLP Layer. After training, the classification heads are discarded and only the LISBET embedding model is kept for subsequent analysis. **c**, Schema of analysis pipeline and visualization of the LISBET embedding in reduced dimension using UMAP after training. The data represented is a random sample ($n = 10000$) of the test set in the CalMS21 - Task 1 dataset (Sun *et al.*, 2021). The position of dots corresponds to LISBET embedding obtained from the time windows analyzed and color overlay corresponds to the independent human annotations. **d**, Same analysis as in **c** ($n = 10000$), but for the CalMS21 - Task 3 dataset (Sun *et al.*, 2021). Behavior labels: m, mount attempt; a, approach; d, disengaged; i, intromission; s, sniff face; w, white rearing; g, groom.

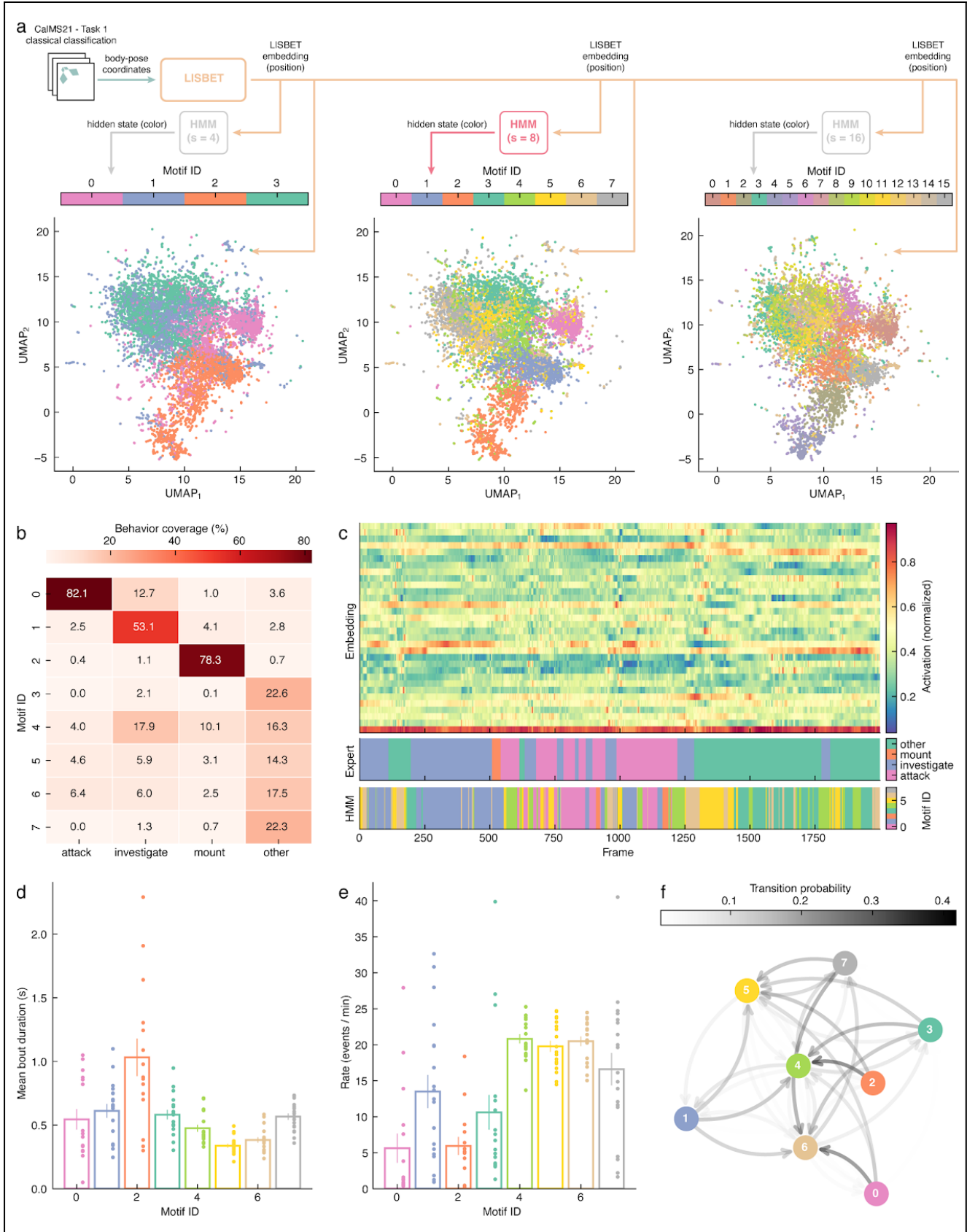


Fig. 2: LISBET embedding segmentation into behavioral motifs. **a**, Schematics of the analysis and segmentation pipeline. Visualization of the LISBET embeddings in 2D via UMAP, segmentation via Hidden Markov Models (HMMs). The data represented is a random sample ($n = 10000$) of the test set in the CalMS21 - Task 1 dataset (Sun *et al.*, 2021). The position of dots corresponds to LISBET embedding obtained from the time windows analyzed (as Fig1c) and color overlay corresponds to social motifs obtained from automatic segmentation of LISBET embedding using HMM with a different number of hidden states ($s = 4$, left; $s = 8$, center; $s = 16$, right). The social

motifs obtained from HMM ($s = 8$) segmentation are used for the analysis in panels (b-f). **b**, Percentage of behavioral coverage of human-annotated behaviors by LISBET motifs **c**, Example of a video segment of 2000 frames showing temporal alignment of corresponding heatmap of LISBET embeddings (activation value of last layer of LISBET backbone, top), with corresponding human annotations (middle) and social motifs obtained from segmentation of LISBET embedding with HMM (bottom). **d**, Mean duration of each social motif. **e**, Rate of each social motif. Mean duration of each behavioral motif. **f**, Transition probability between social motifs.

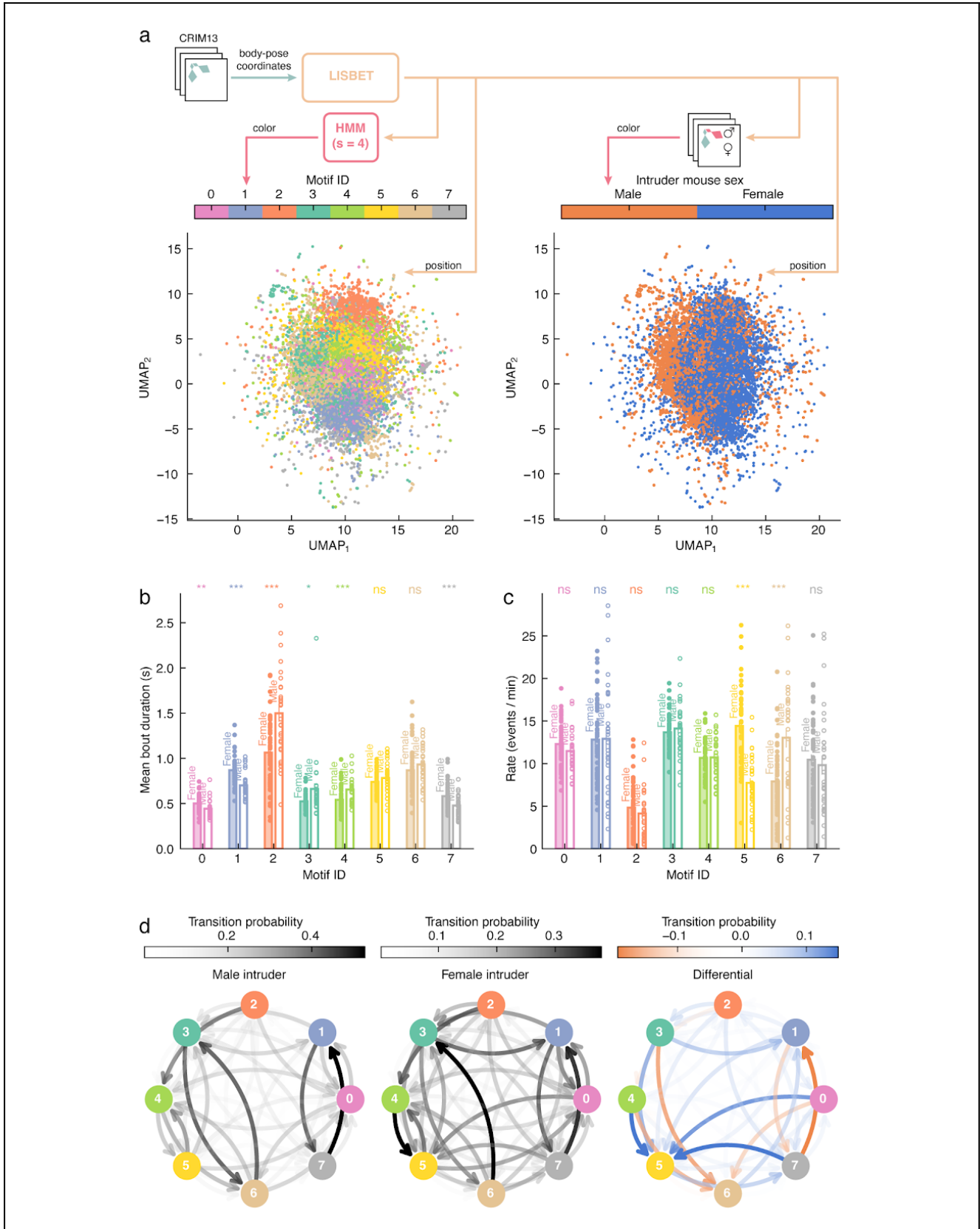


Fig. 3: Behavioral phenotyping using LISBET. **a**, Schematics of the analysis and segmentation pipeline for group comparisons. Visualization of the LISBET embeddings in 2D via UMAP, segmentation via Hidden Markov Models (HMMs). The data represented is a random sample ($n = 10000$) of the CRIM13 dataset (Burgos-Artizzu *et al.*, 2012). The position of dots corresponds to LISBET embedding obtained from the time windows analyzed (as Fig1c) and color overlay corresponds to social motifs obtained from automatic segmentation of LISBET embedding using HMM with eight hidden states. **b**, Mean duration of social motifs in each group. **c**, Rate of social motifs in each group. **d**, Transition probability between social motifs in the male vs male case (left), male vs female (middle), and differential case (female-male, right).

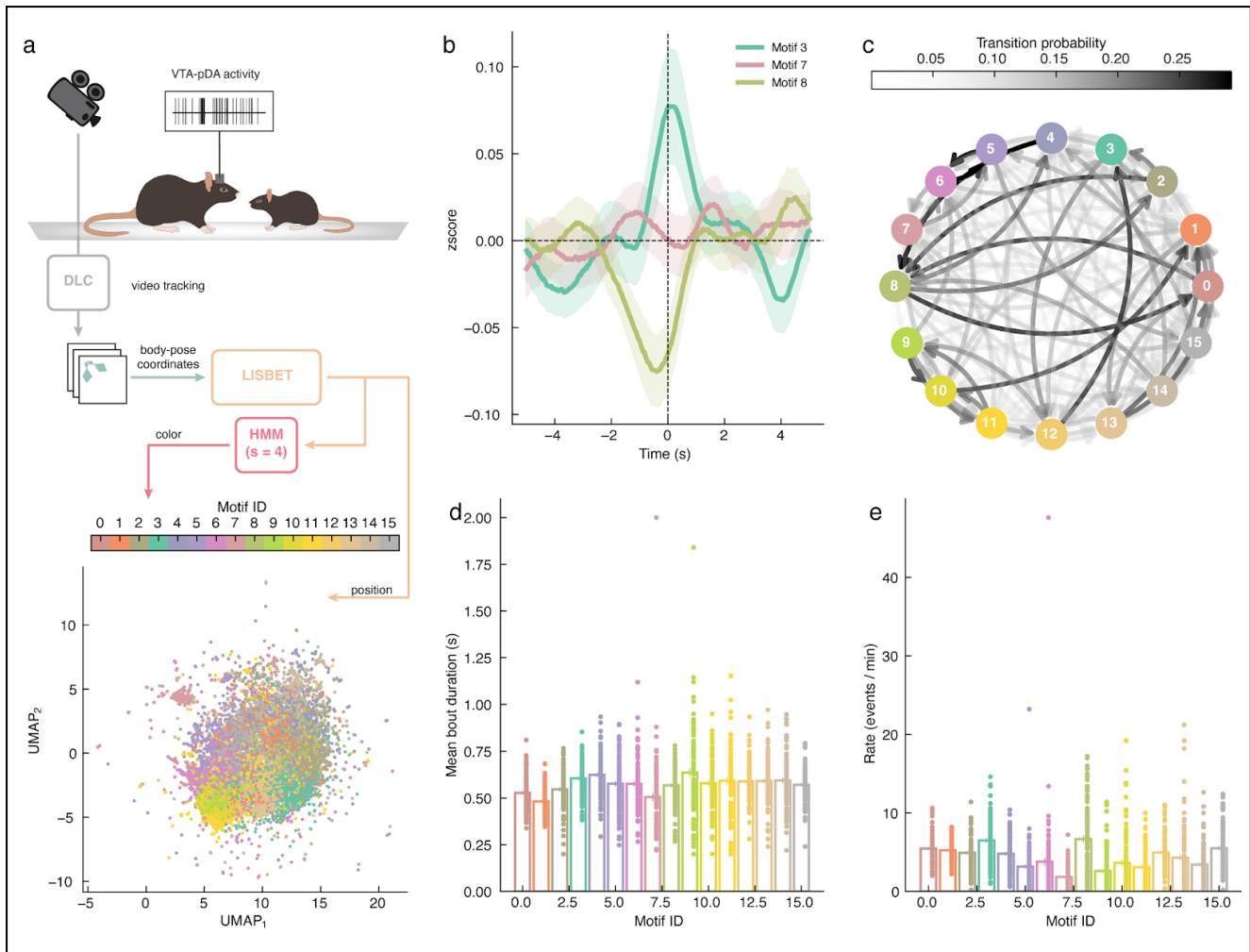


Fig. 4: VTA-pDA neuron activities correlate with different social motifs obtained from segmentation of LISBET embedding **a**, Schema of analysis pipeline and visualization of the LISBET embedding in reduced dimension using UMAP after training and segmentation. Data represented is from video recordings of 2 mice interacting together followed by tracking using DeepLabCut. Spike unit of putative dopaminergic neurons in the ventral tegmental area (VTA-pDA neurons) is also recorded but not used to obtain automatic segmentation of social motifs. Position of dots corresponds to LISBET embedding obtained from the time windows analyzed and color overlay corresponds to social motifs obtained from automatic segmentation of LISBET embedding using HMM with sixteen hidden states. **b**, Perievent Time Histogram (PETH) of the normalized frequency (z score) of VTA-pDA neurons time-locked to three examples of social motifs correlated with diverging neuronal activities. **c**, Transition probability between social motifs. **d**, Mean duration of each social motif. **e**, Rate of each social motif.

Acknowledgements

The authors would like to acknowledge Alexandre Pouget and Charles Findling for helping conceptualize the Next Window Prediction (NWP) task and for discussions on the network training process. Bastien Redon for suggestions on the manuscript. Andrea Della Valle for discussions on the model.

The authors would also like to acknowledge the use of ChatGPT, a language model developed by OpenAI, as a tool to enhance language quality and to facilitate discussions on the topics covered in this research. ChatGPT was employed for language improvement and general linguistic assistance during the writing process. It is important to note that while ChatGPT has been a valuable resource, the final content, interpretation of results, and the conclusions drawn in this paper were the authors' responsibility. The tool was used to aid in drafting and refining the manuscript but did not contribute to the scientific methodology or analysis of the research. The authors appreciate the availability of this resource, which helped enhance the clarity and precision of the language used in this manuscript.

Contributions

G.C., B.G., and C.B. conceived the study. G.C. designed the model. B.G. performed the in vivo experiments. G.C., B.G., and C.B. wrote the manuscript.

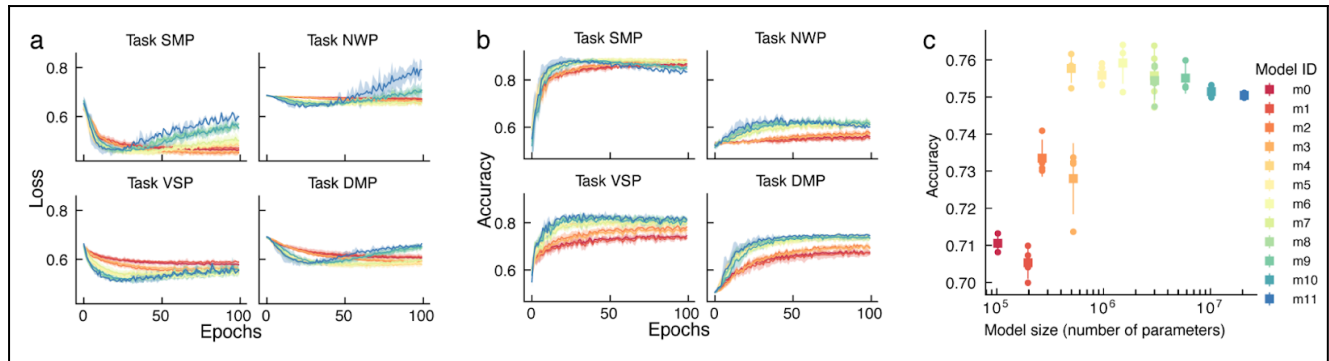
References

- Arnab, A. *et al.* (2021) 'ViViT: A Video Vision Transformer', *arXiv:2103.15691 [cs]* [Preprint]. Available at: <http://arxiv.org/abs/2103.15691> (Accessed: 1 June 2021).
- Bohnslav, J.P. *et al.* (2021) 'DeepEthogram, a machine learning pipeline for supervised behavior classification from raw pixels', *eLife*, 10, p. e63377. Available at: <https://doi.org/10.7554/eLife.63377>.
- Burgos-Artizzu, X.P. *et al.* (2012) 'Social behavior recognition in continuous video', in *2012 IEEE Conference on Computer Vision and Pattern Recognition. 2012 IEEE Conference on Computer Vision and Pattern Recognition*, pp. 1322–1329. Available at: <https://doi.org/10.1109/CVPR.2012.6247817>.
- de Chaumont, F. *et al.* (2019) 'Real-time analysis of the behaviour of groups of mice via a depth-sensing camera and machine learning', *Nature Biomedical Engineering*, 3(11), pp. 930–942. Available at: <https://doi.org/10.1038/s41551-019-0396-1>.
- Chollet, F. and others (2015) 'Keras'. Available at: <https://keras.io>.
- Devlin, J. *et al.* (2019) 'BERT: Pre-training of Deep Bidirectional Transformers for Language Understanding', *arXiv:1810.04805 [cs]* [Preprint]. Available at: <http://arxiv.org/abs/1810.04805> (Accessed: 28 May 2021).
- Dosovitskiy, A. *et al.* (2020) 'An Image is Worth 16x16 Words: Transformers for Image Recognition at Scale', *arXiv:2010.11929 [cs]* [Preprint]. Available at: <http://arxiv.org/abs/2010.11929> (Accessed: 1 June 2021).
- Dunn, T.W. *et al.* (2021) 'Geometric deep learning enables 3D kinematic profiling across species and environments', *Nature Methods*, 18(5), pp. 564–573. Available at: <https://doi.org/10.1038/s41592-021-01106-6>.
- Harris, C.R. *et al.* (2020) 'Array programming with NumPy', *Nature*, 585(7825), pp. 357–362. Available at: <https://doi.org/10.1038/s41586-020-2649-2>.
- hmmlearn, team (2014) *hmmlearn/hmmlearn: Hidden Markov Models in Python, with scikit-learn like API*. Available at: <https://github.com/hmmlearn/hmmlearn> (Accessed: 5 November 2023).
- Hsu, A.I. and Yttri, E.A. (2021) 'An Open Source Unsupervised Algorithm for Identification and Fast Prediction of Behaviors', *bioRxiv*, p. 770271. Available at: <https://doi.org/10.1101/770271>.
- Hunter, J.D. (2007) 'Matplotlib: A 2D Graphics Environment', *Computing in Science & Engineering*, 9(3), pp. 90–95. Available at: <https://doi.org/10.1109/MCSE.2007.55>.
- Kluyver, T. *et al.* (2016) 'Jupyter Notebooks – a publishing format for reproducible computational

- workflows', in F. Loizides and B. Schmidt (eds) *Positioning and Power in Academic Publishing: Players, Agents and Agendas*. IOS Press, pp. 87–90.
- Lauer, J. *et al.* (2022) 'Multi-animal pose estimation, identification and tracking with DeepLabCut', *Nature Methods*, pp. 1–9. Available at: <https://doi.org/10.1038/s41592-022-01443-0>.
- Luxem, K. *et al.* (2022) 'Identifying behavioral structure from deep variational embeddings of animal motion', *Communications Biology*, 5(1), pp. 1–15. Available at: <https://doi.org/10.1038/s42003-022-04080-7>.
- Marks, M. *et al.* (2022) 'Deep-learning based identification, tracking, pose estimation, and behavior classification of interacting primates and mice in complex environments'. bioRxiv, p. 2020.10.26.355115. Available at: <https://doi.org/10.1101/2020.10.26.355115>.
- Martín Abadi *et al.* (2015) 'TensorFlow: Large-Scale Machine Learning on Heterogeneous Systems'. Available at: <https://www.tensorflow.org/>.
- Mathis, A. *et al.* (2018) 'DeepLabCut: markerless pose estimation of user-defined body parts with deep learning', *Nature Neuroscience*, 21(9), pp. 1281–1289. Available at: <https://doi.org/10.1038/s41593-018-0209-y>.
- McInnes, L., Healy, J. and Melville, J. (2020) 'UMAP: Uniform Manifold Approximation and Projection for Dimension Reduction', *arXiv:1802.03426 [cs, stat]* [Preprint]. Available at: <http://arxiv.org/abs/1802.03426> (Accessed: 2 March 2021).
- McKinney, W. (2010) 'Data Structures for Statistical Computing in Python', in S. van der Walt and J. Millman (eds) *Proceedings of the 9th Python in Science Conference*, pp. 56–61. Available at: <https://doi.org/10.25080/Majora-92bf1922-00a>.
- Nilsson, S.R. *et al.* (2020) 'Simple Behavioral Analysis (SimBA) – an open source toolkit for computer classification of complex social behaviors in experimental animals', *bioRxiv*, p. 2020.04.19.049452. Available at: <https://doi.org/10.1101/2020.04.19.049452>.
- Pedregosa, F. *et al.* (2011) 'Scikit-learn: Machine Learning in Python', *Journal of Machine Learning Research*, 12, pp. 2825–2830.
- Pereira, T.D. *et al.* (2020) 'SLEAP: Multi-animal pose tracking', *bioRxiv*, p. 2020.08.31.276246. Available at: <https://doi.org/10.1101/2020.08.31.276246>.
- Pereira, T.D., Shaevitz, J.W. and Murthy, M. (2020) 'Quantifying behavior to understand the brain', *Nature Neuroscience*, 23(12), pp. 1537–1549. Available at: <https://doi.org/10.1038/s41593-020-00734-z>.
- Segalin, C. *et al.* (2021) 'The Mouse Action Recognition System (MARS) software pipeline for automated analysis of social behaviors in mice', *eLife*. Edited by G.J. Berman, K.M. Wassum, and A. Gal, 10, p. e63720. Available at: <https://doi.org/10.7554/eLife.63720>.
- Sun, J.J. *et al.* (2021) 'The Multi-Agent Behavior Dataset: Mouse Dyadic Social Interactions', *arXiv:2104.02710 [cs]* [Preprint]. Available at: <http://arxiv.org/abs/2104.02710> (Accessed: 4 June 2021).
- Van Rossum, G. and Drake Jr, F.L. (1995) *Python reference manual*. Centrum voor Wiskunde en Informatica Amsterdam.
- Virtanen, P. *et al.* (2020) 'SciPy 1.0: Fundamental Algorithms for Scientific Computing in Python', *Nature Methods*, 17, pp. 261–272. Available at: <https://doi.org/10.1038/s41592-019-0686-2>.
- Wiltschko, A.B. *et al.* (2020) 'Revealing the structure of pharmacobehavioral space through motion sequencing', *Nature Neuroscience*, 23(11), pp. 1433–1443. Available at: <https://doi.org/10.1038/s41593-020-00706-3>.
- Ye, S. *et al.* (2023) 'AmadeusGPT: a natural language interface for interactive animal behavioral analysis'. arXiv. Available at: <https://doi.org/10.48550/arXiv.2307.04858>.

Supplementary Information

Supplementary Figures



S1: LISBET tuning results. **a**, Evolution of dev set losses during training for each self-supervised task. Solid lines represent the mean loss across cross-validation folds while the shaded areas represent the corresponding standard deviation. Model ID color codes as in **c**. **b**, Evolution of dev set binary accuracy during training for each self-supervised task. Solid lines and shaded areas have the same meaning as in **b**, Model ID color codes as in **c**. **c**, Binary accuracy summary. Circles represent the mean of the last 5 epochs in each cross-validation fold. Squares and vertical lines represent the mean and standard deviation across cross-validation folds respectively. Sample size $n = 4$ for every model, except model m9 with $n = 3$ and model m11 with $n = 2$.

Supplementary Tables

emb_dim	num_layers	num_heads	hidden_dim	num_params	accuracy			loss		
					mean	std	count	mean	std	count
16	2	2	512	102484	0.710577	0.002083	4	2.318696	0.011801	4
			1024	196180	0.705298	0.004305	4	2.345877	0.013539	4
	4	4	1024	266100	0.733517	0.004996	4	2.261308	0.012311	4
			2048	521076	0.727986	0.009574	4	2.280054	0.038062	4
32	4	4	1024	498404	0.757685	0.003869	4	2.271098	0.018075	4
			2048	966372	0.755885	0.003045	4	2.301716	0.008641	4
	8	8	2048	1516388	0.759156	0.005563	4	2.292438	0.021070	4
			4096	2984804	0.755733	0.007679	4	2.319103	0.042857	4
64	8	8	2048	3006148	0.754422	0.005126	4	2.460503	0.026182	4
			4096	5850820	0.755084	0.004153	3	2.464478	0.037181	3
	16	16	4096	10213572	0.751449	0.001542	4	2.481167	0.042597	4
			128	16	16	4096	20734340	0.750459	0.000940	2

S1: LISBET tuning summary results.